

See discussions, stats, and author profiles for this publication at: <https://www.researchgate.net/publication/7483863>

Building three-dimensional images using a time-reversal chaotic cavity

Article in IEEE Transactions on Ultrasonics Ferroelectrics and Frequency Control · October 2005

DOI: 10.1109/TUFFC.2005.1516021 · Source: PubMed

CITATIONS

23

READS

33

4 authors, including:



Mickaël Tanter

École Supérieure de Physique et de Chimie Industrielles

492 PUBLICATIONS 12,784 CITATIONS

SEE PROFILE

Some of the authors of this publication are also working on these related projects:



Visual Cortex fUS Imaging [View project](#)



Hemodynamics correlates of Theta Rhythm [View project](#)

All content following this page was uploaded by [Mickaël Tanter](#) on 15 April 2016.

The user has requested enhancement of the downloaded file. All in-text references [underlined in blue](#) are added to the original document and are linked to publications on ResearchGate, letting you access and read them immediately.

Building Three-Dimensional Images Using a Time-Reversal Chaotic Cavity

Gabriel Montaldo, Delphine Palacio, Mickael Tanter, and Mathias Fink

Abstract—The design of two-dimensional (2-D) arrays for three-dimensional (3-D) ultrasonic imaging is a major challenge in medical and nondestructive applications. Thousands of transducers are typically needed for focusing and steering in a 3-D volume. In this article, we propose a different concept allowing us to obtain electronic 3-D focusing with a small number of transducers. The basic idea is to couple a small number of transducers to a chaotic reverberating cavity with one face in contact with the body of the patient. The reverberations of the ultrasonic waves inside the cavity create at each reflection virtual transducers. The cavity acts as an ultrasonic kaleidoscope multiplying the small number of transducers and creating a much larger virtual transducer array. By exploiting time-reversal processing, it is possible to use collectively all the virtual transducers to focus a pulse everywhere in a 3-D volume. The reception process is based on a nonlinear pulse-inversion technique in order to ensure a good contrast. The feasibility of this concept for the building of 3-D images was demonstrated using a prototype relying only on 31 emission transducers and a single reception transducer.

I. INTRODUCTION

IN 2-D conventional ultrasonography, the diagnostician is limited in the visualization of some diseases because he must integrate many 2-D images to reconstruct mentally a 3-D volume. Over the past few years, advances in technology that include high-speed computing, array technology, and storage hardware have permitted us to build 3-D ultrasound imaging systems [1], [2]. Two different approaches have been investigated to build a complete 3-D image. The first type of 3-D ultrasound system uses a series of 2-D images produced by a conventional 1-D array [3], [4]. The 1-D array is moved by the practitioner or by a motorized device in the direction perpendicular to the image plane to get a volumetric data acquisition. The scanning sequence requires a position sensor in order to know precisely the position and angulations of each slice. The 3-D ultrasound data set and the position data set are necessary to reconstruct the 3-D image. The main disadvantages of this method are the sensitivity of the 3-D reconstruction to the accuracy of position data and to the artifacts caused by respiratory motion and the low frame rates limited by the mechanical scanning.

The second type of 3-D ultrasound systems uses new generations of 2-D arrays of transducers [5]–[8] in order to focus an ultrasonic pulse in a 3-D volume. This approach

is the most convenient for the practitioner as the scanning of the complete volume is achieved electronically, and it should produce images of better quality at higher frame rate than a mechanical scanning. Unfortunately, this technique involves a lot of new technological problems: the high number of elements (thousands in some cases) requires a complex and expensive electronic multiplexing. Moreover, the small size of the individual elements increases the electrical mismatch and results in a reduced sensitivity. And, the wiring of thousands of elements is a major technological challenge.

Here, we present an original approach that replaces the 2-D array by a set of less than 100 elements. Our solution combines the use of time reversal technology with a small number of piezoelectric transducers fastened to a reverberating solid cavity presenting one face in contact with the investigated medium. Time-reversal focusing was studied previously in the field of ultrasound [9], for medical applications [10], and in ocean acoustics [11]. This technique is based on the reversibility of acoustic propagation, which implies that the time-reversed version of an incident pressure field naturally refocuses in space and time on its source, whatever the heterogeneity of the propagation medium. More precisely, it means that, for every burst of sound emitted from a source and possibly reflected and refracted by multiple boundaries, there exists a set of waves that precisely retraces all the complex path and converges to the original source, as if time were going backward. This idea leading to the concept of time-reversal pulse recompression in reverberating medium has been successfully applied in solid waveguides for shock wave lithotripsy [12]. In such a configuration, one face of the waveguide is in contact with the patient's body while a small number of transducers is glued on the opposite face. Thanks to the multiple reverberations on the waveguide boundaries, waves emitted by each transducer are multiply reflected, creating at each reflection virtual transducers that can be observed from the desired focal point. Thus, we create a large virtual array from a limited number of transducers. The result of such an operation is that a small number of transducers is multiplied to create a kaleidoscopic transducer array. However, symmetries implied in waveguides create periodic kaleidoscopic arrays, resulting in grating lobes that limit the interest of this technique to shock wave generation for lithotripsy. To extend this concept to pulse-echo imaging, sidelobes have to be strongly reduced. The solution we propose is to break the waveguide's symmetries by introducing reverberating media with chaotic geometries such as chaotic billiards. Preliminary works on

Manuscript received July 29, 2004; accepted January 27, 2005.

The authors are with the Laboratoire Ondes et Acoustique, 75005 Paris France (e-mail: gabrielmontaldo@yahoo.fr).

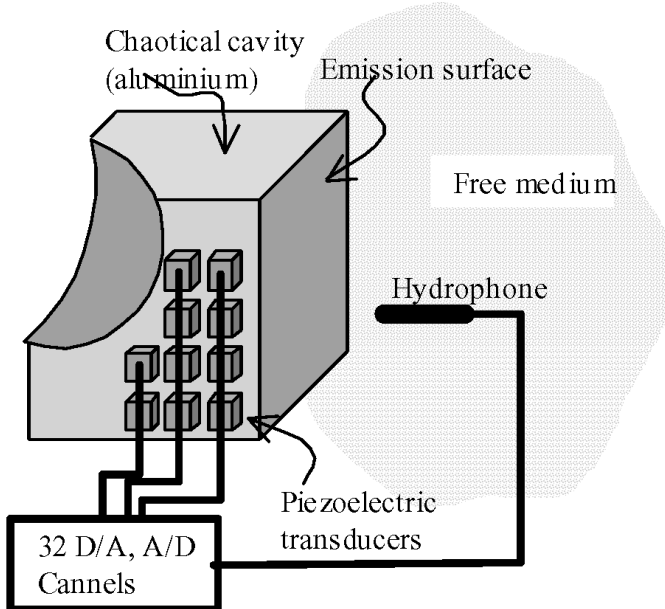


Fig. 1. Experimental setup. The main part of the kaleidoscope consists of a chaotic cavity made of aluminum with 31 piezoelectric transducers glued on one face. The transducers are 8 by 5 mm rectangular piezoelectric ceramics and work at a central frequency of 1.5 MHz. Each transducer is connected to an independent digital-to-analog and analog-to-digital channel. One face of the kaleidoscope is in contact with a fluid medium in order to perform the calibration. Once the system is calibrated, this same face then is put in contact with the tissue medium to image.

time reversal in 2-D closed cavities was done by Draeger *et al.* [13], [14] using Bunimovitch billiards. Here, we extend this work to 3-D leaky cavities and we select a Sinai billiard geometry to achieve 3-D focusing. A Sinai billiard is a cube with a spherical hole in the middle. A beam reflected by the faces of this cavity has the propriety of passing as close as you want from any arbitrary point in the cavity. In other words, the beam goes through all the points of the cavity. In order to simplify the building we use 1/8th of this billiard, which looks like a cube with a bitten corner of spherical shape (see Fig. 1).

In the first part of this article, we present a prototype of such a kaleidoscope and the experimental results obtained with various methods, time reversal, 1-bit time reversal, and nonlinear techniques. In particular, we show how the complexity of 2-D arrays technology is here transferred into the spatio temporal codes stored in memories. In the second part of the article, we show some simple images of 3-D objects using a prototype made of 31 emission transducers and a single reception transducer.

II. FOCUSING A PULSE IN 3-D WITH A TIME-REVERSAL KALEIDOSCOPE

The pioneer prototype system is made of a solid chaotic aluminum cavity (a 3-D Sinai billiard of $50 \times 50 \times 50 \text{ mm}^3$) with 31 transmit elements glued on one surface. The transmitters are 8 by 5 mm rectangular piezoelectric ceramics

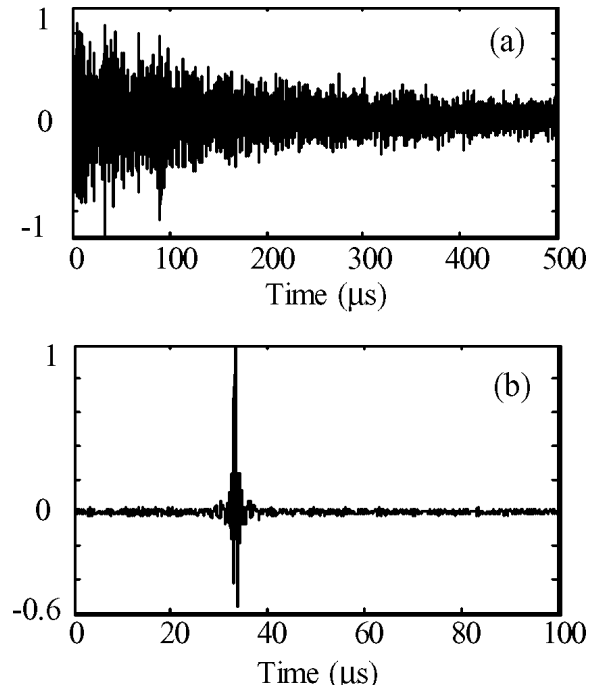


Fig. 2. (a) Signal recorded on one transducer element of the kaleidoscope after sending a pulse of $1 \mu\text{s}$ at the desired location. Due to the multiple reflections on the faces of the cavity, the signal duration is very long. (b) Time-reversal recompression in the hydrophone. The original brief pulse is recovered with some side lobes.

with a 1.5 MHz central frequency. One of the surfaces is in contact with the medium to image (see Fig. 1). Each transducer is connected to a fully programmable, multi-channel electronic system relying on a 32 MHz sampling frequency and a 80 Vpp excitation.

In order to focus a short pulse inside the medium, we use the time-reversal process. A time-reversal (TR) experiment is divided in two steps.

- First, an ultrasonic source located in the medium to image (here an homogeneous fluid mimicking human tissues) at the chosen focal point sends a short ultrasonic pulse (typically $1 \mu\text{s}$ duration) centered around 1.5 MHz. The acoustic waves propagate in the medium and penetrate inside the solid cavity. Due to the strong reverberations inside the cavity, the waves are reflected hundreds of times and the impulse responses $h_i(t)$ received by the i^{th} transducer last a very long time [up to $500 \mu\text{s}$, Fig. 2(a)]. It corresponds to about 1.5 m of reverberant propagation in aluminum corresponding to nearly 300 reflections on the cavity boundaries.¹
- In the second step, the received signals are time reversed and $h_i(-t)$ is sent back from each transducer of the cavity. The waves perform the inverse way, and they eventually focus at the initial source point both in

¹Note that, thanks to spatial reciprocity of wave propagation, this first step can be achieved using a hydrophone instead of an acoustic transmitter at focus. The Green's function then is acquired by emitting successively with each transducer glued on the cavity and recording the resulting echo on the hydrophone at focus. This approach is more efficient in terms of sensitivity.

space and time exactly as if time was going backward. Fig. 2(b) represents the time-reversed pulse received at the initial source location. The initial pulse duration ($1 \mu\text{s}$) is recovered, and this phenomenon can be named the time-reversal temporal recompression.

This process achieved in a calibration medium like water allows us to learn the temporal codes to be applied on each transducer in order to focus at a given location. By repeating this process for different initial source locations, we can learn the coded signals $h_i(-t)$ allowing us to focus on any specific point of the medium. The complete calibration of the kaleidoscope consists in recording all the data set of coded signals needed to focus at each point of the calibration medium.

This process was modeled using a numerical simulation of the wave propagation. This numerical approach greatly helps us to understand the building of the time-reversed focused beam. We performed a 2-D finite differences time domain simulation (FDTD) taking into account longitudinal and transverse waves contributions in the solid, mode conversions, and longitudinal waves propagation in the calibration fluid. The solid has free boundaries (air interface) and the fluid presents perfect absorbing boundaries.

Fig. 3 shows the amplitude of the displacement at different time steps during the backpropagation of the time-reversed wavefront. The impulse responses $h_i(t)$ already have been simulated in the first part of the time-reversal numerical experiment. Here, the signals $h_i(-t)$ are sent by each transducer of the cavity. In Fig. 3(a), $-206 \mu\text{s}$ before the focusing time, a lot of energy is injected in the cavity, and a very low and incoherent noise is leaking out of the cavity. At $-34 \mu\text{s}$, the reverberations begin to build a spherical wavefront inside the cavity [Fig. 3(b)]. The spherical wave front is clearly defined at $-36 \mu\text{s}$ [Fig. 3(c)] and it leaves the cavity at $-27 \mu\text{s}$ [Fig. 3(d)]. At $0 \mu\text{s}$, it focuses at the initially chosen location [Fig. 3(e)]. As one can notice in Fig. 3(b), the central part of the wavefront is due to longitudinal waves in the solid cavity, whereas the edges of the wavefront correspond to transverse wave contributions. Longitudinal waves in Fig. 3(b) are late in comparison with transverse waves but overtake their delay on transverse waves at the exact time they leave the cavity. Thus, transverse waves are shown to contribute to high angular frequencies of the focusing beam, and longitudinal waves contribute to low angular frequencies of the beam. It is nice to see how elegantly time reversal takes benefit from mode conversions in order to overcome the critical angle limitation suffered by longitudinal waves.

A. One Bit Time Reversal and Nonlinear Harmonic Focusing

The calibration process to focus in a complete 3-D large volume requires a very large memory for the storage of the codes. In our system, based on 31 transducers and $500 \mu\text{s}$ signals sampled at 32 MHz, the waveforms required for each focal point correspond to 992 Kbytes of memory. A

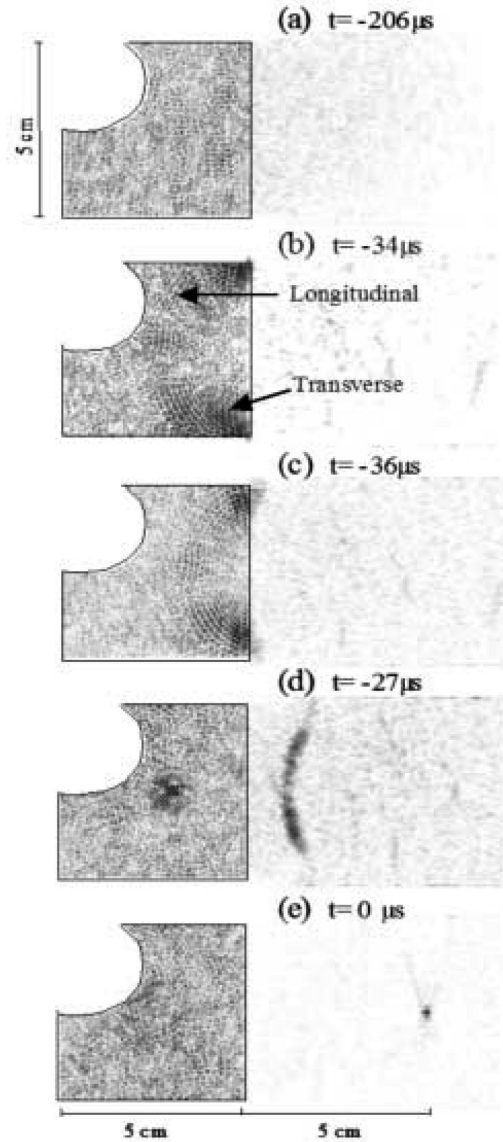


Fig. 3. Numerical simulation of a time-reversal focusing experiment. (a) The transducers begin to emit their coda. Only a very low incoherent noise is leaving the cavity. (b) and (c) A spherical wave is progressively built inside the cavity. In (b) the longitudinal waves are in advance respect to transverse waves. (d) The spherical wave is transmitted to the medium. (e) Spatial and temporal focusing at the desired location.

way to reduce memory is to use a 1-bit time-reversal focusing (1bit-TR). In this 1-bit approach, we transmit only a signal of constant amplitude on each transducer with two possible (phases 0 or π). The transmitted signals then are proportional to $sign(h_i(-t))$. As it was seen in a previous study [15], in a complex reverberating medium like a chaotic cavity, the simpler 1bit-TR surprisingly refocuses the pulsed wavefront with the same quality as the complete time-reversal process applied both to phase and amplitude of signals. The focal spot characteristics (pulse duration and noise level) are equivalent, even if the data set of transmit codes loses its amplitude information. As the instantaneous phase of the transmit signals convey the most important part of the information, the focusing is com-

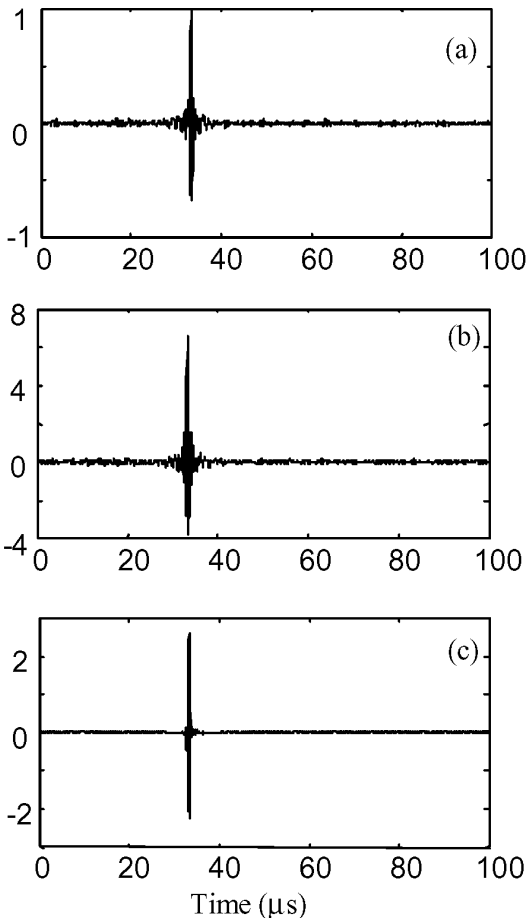


Fig. 4. (a) 8-bit time-reversal focusing. The amplitude of this figure is normalized to 1, the other graphics are plotted using the same scale. (b) 1-bit time-reversal focusing. The amplitude is six times bigger than the 8-bit focusing, and the sidelobes have the same level. (c) Pulse-inversion focusing with 1-bit time reversal. The sidelobes almost disappeared because the low amplitude of sidelobes is not sufficient to generate nonlinear harmonics.

parable and it allows us to store only 110 Kb of memory per point. Moreover, as the 1-bit transmit signal contains more energy than the true signal, the focused pulse has a higher amplitude [12], resulting in a stronger sensitivity. In Fig. 4(b), we can see the focused pulse using a 1bit-TR experiment. The pulsed signal received at focus is very similar to the complete TR focusing experiment presented in Fig. 4(a), but the peak amplitude is 6.6 times higher.

B. Nonlinear Imaging

Using a cavity with 31 transducers, the temporal recompression of the time-reversal process is not perfect, and residual sidelobes remain around the main pulse as can be seen in Figs. 4(a) and (b). We can define the signal/sidelobe ratio as $ss = \text{pulse_amplitude}/\text{sidelobe_amplitude}$. As said in the previous section, we observe a similar ss for both TR and 1bit-TR, reaching nearly -35 dB. This ss is not high enough to build a good echographic image of a complex media like biological tissues. In a random scattering medium, such

temporal sidelobes give rise to a strong speckle noise that can decrease the image contrast quality.

In order to overcome this problem, we propose to take benefit of nonlinear effects occurring during the wave propagation of the time-reversed signals outside of the cavity. An extensive literature shows that the nonlinear effects induced by the natural propagation in human tissues [16]–[18] or by the injection of some contrast agents [19], [20] can be used to improve the image quality.

During the time-reversal focusing experiment, the amplitude of the time-reversed wavefront outside of the cavity is sufficient to generate significant nonlinear effects along the beam path. As the harmonics generation depends roughly on the square of the wave amplitude, the low noise level noise outside the main temporal focal spot is too weak to generate a significant amount of harmonics contrary to the pulsed peak signal.

Of course, the observation of the harmonics that are generated depends on the initial bandwidth of the transmitted signal. With a narrowband initial pulse, it is easy to isolate the second harmonic of the signal using a bandpass filter as the second harmonic, and fundamental frequencies are well separated. On the contrary, for a wideband signal, the second harmonic is mixed with the fundamental signal, and it is better to use a classical-two step pulse inversion (PI) technique. In the well-known PI technique, we first send a pulse and later its opposite. If the propagation is linear, the sum of the backscattered echoes corresponding to these two steps gives zero. But if there are some nonlinear effects during the propagation, the addition clears up the linear part and only the nonlinear component remains.

In Fig. 4(c) we can see the PI signal detected at the focal point. The temporal compression of this harmonic signal presents temporal sidelobes at -60 dB showing a gain of 25 dB compared to the fundamental signal. This result shows the excellent temporal focusing of the PI technique. In order to examine the spatial focusing, a hydrophone is moved along a line [see setup in Fig. 5(a)] to represent in a time-space mode (B-scan) both the space and time focusing pattern. In Figs. 5(a) and (b), we can see a B-scan using, respectively, 1bit-TR and 1bit-TR with PI. If the hydrophone is moved in a 2-D plane parallel to the surface of the cavity [elevation plane, see setup in Fig. 5(c)], we can scan the maximum pressure amplitude at each point and map the bidimensional spatial focusing (C-scan). Figs. 5(c) and (d) show the C-scan for 1bit-TR and 1bit-TR with PI. The comparison of these figures clearly shows that the use of the second harmonic permits a better spatial focusing with a nearly -50 dB contrast.

Fig. 6 shows the ability of the system of focusing in different points. The time-reversal focusing process has been performed at different locations separated by 10 mm. The focusing contrast for each point is very similar (about -50 dB for the time-reversal PI method).

The resolution of the system is due to the geometrical aperture of the emission surface of the cavity. As the wave leaving the cavity is a spherical one, the lateral resolution is that of a 2-D matrix of the same geometrical aperture

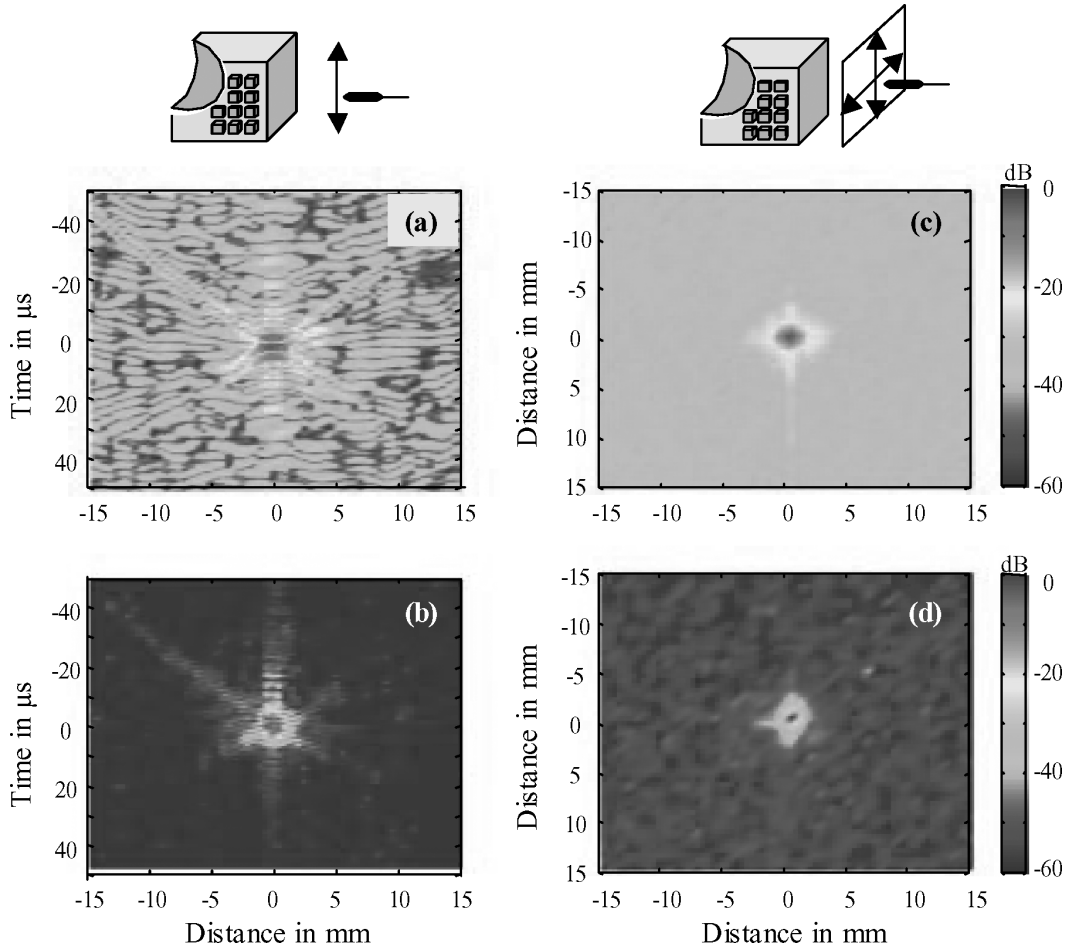


Fig. 5. (a) Spatiotemporal focusing using time-reversal. The hydrophone moves along a line parallel to the surface of the kaleidoscope as is shown in schemas. (b) Spatiotemporal nonlinear focusing using the PI technique combined with time reversal. (c) Bidimensional spatial focusing using classical time reversal; the figure displays the maximum amplitude at each location in a plane parallel to the surface of the kaleidoscope (see schema). (d) Bidimensional spatial focusing using the PI technique combined with time reversal. The PI technique clearly gives a better focusing quality with a nearly -60 dB sidelobe level.

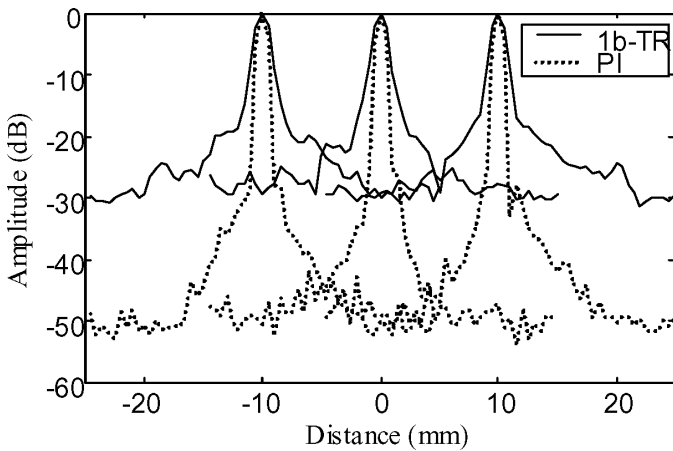


Fig. 6. Focusing at different locations using a 1-bit time-reversal technique with (solid line) and without PI (dotted line). The focusing quality is very similar at each location.

$\lambda f/D$ with f the focal depth and D the size of the array. With an aperture of 50 mm and a focal depth of 80 mm, the theoretical resolution is 1.6 mm, and the measured resolution in Fig. 6 is 1.7 mm.

C. Study of the Signal/Sidelobes

The global contrast obtained using the ultrasonic kaleidoscope depends on the transducers bandwidth and the number of elements. We can estimate the contrast of the focused pulse using some simple approximations. We define the ss = signal/sidelobe ratio as:

$$ss = \text{Maximum_pulse_amplitude} / \text{sidelobe_amplitude}. \tag{1}$$

If n transducers are used in the transmit mode and send a set of signals $e_i(t) i = 1..n$, the signal $r(t)$ received at a given location in the medium is given by:

$$r(t) = \sum_{i=1}^n h_i(t) \otimes e_i(t), \tag{2}$$

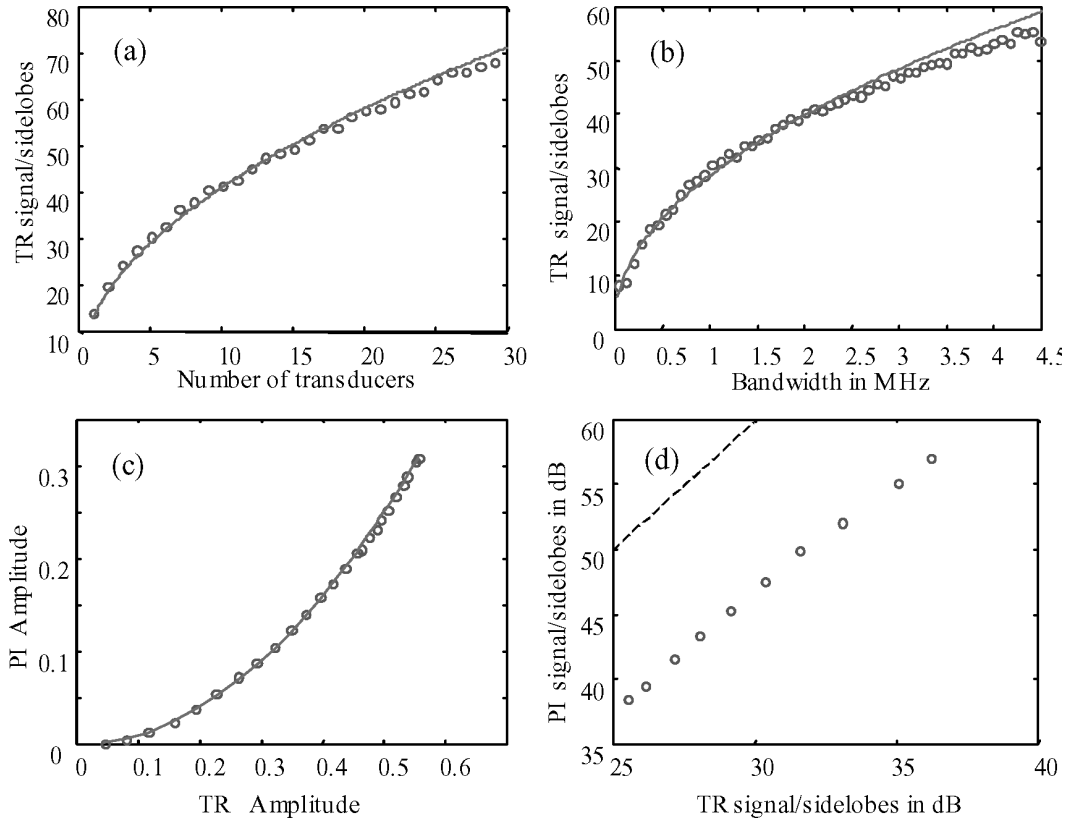


Fig. 7. (a) Time-reversal signal/sidelobes versus the number of transducers. The dots are the experimental data, the line is a square root fitting. (b) Time-reversal signal/sidelobes versus bandwidth of the transducer. The dots are the experimental data, and the line is a square root fitting. A wideband transducer center at 3-MHz was used. (c) Pulse inversion amplitude versus the time-reversal amplitude. The line is the quadratic model and the dots are the experimental measures. (d) Pulse inversion contrast versus time-reversal signal/sidelobes, both in a decibel scale. The model (line) is 12 dB higher than the experimental data (dots). This deviation is due to quantification errors of our electronics in the transmit mode.

where $h_i(t)$ is the impulse response between the i^{th} transducer and the chosen location.

In a time-reversal focusing experiment, the emission signals correspond to $e_i(t) = h_i(-t)$. Accordingly, the signal received at focus becomes:

$$r(t) = \sum_{i=1}^n r_i(t) = \sum_{i=1}^n h_i(t) \otimes h_i(-t). \quad (3)$$

At $t = 0$, each component $r_i(0)$ is a positive number, and they added coherently in (3). So, the amplitude of the final pulse is proportional to the number of transducers n .

At $t \neq 0$, the different signals $r_i(t)$ are not correlated according to the fact that, in a chaotic cavity, the different impulse responses $h_i(t)$ are uncorrelated. This is the so-called spatial diversity of the wave propagation. Consequently, in (3), these signals are added incoherently, and the amplitude of the lobes is proportional to \sqrt{n} . So, the signal/sidelobe of a time-reversal focusing process in the linear regime is proportional to the square root of the number of transducers:

$$ss_{TR} \propto \sqrt{n}. \quad (4)$$

In Fig. 7(a) we can see the experimental signal/sidelobes obtained versus the number of transducers

used in the focusing time-reversal process, and this curve is in good agreement with the square root model.

Another important parameter is the bandwidth of the transducers. Indeed, a large bandwidth allows us to create the same effect as using different spatially uncorrelated transducers. We can define the correlation bandwidth $\delta\omega$ as the frequency separation required between two frequency components to generate two decorrelated acoustical fields in the medium of interest. We can divide the total band $\Delta\omega$ of the transducers in p subbandwidths of length $\delta\omega$ in which $\Delta\omega = p\delta\omega$. In a chaotic cavity as well as in strongly reverberating environments [21], $\delta\omega$ is smaller than in a regular cavity, and the number of decorrelated subbands is maximized. We can take benefit of this frequency diversity.

The impulse response $h(t)$ of the transducer can be decomposed as $h(t) = \sum_{j=1}^p \tilde{h}_j(t)$ where each $\tilde{h}_j(t)$ is the impulse response of one subbandwidth. Performing the time-reversal focusing process, we obtain:

$$r(t) = \sum_{j=1}^p \tilde{r}_j(t) = \sum_{j=1}^p \tilde{h}_j(t) \otimes \tilde{h}_j(-t). \quad (5)$$

In analogy with the case of different transducers, the amplitude of the pulse at $t = 0$ is added coherently and is

proportional to the number of subbands p . But at $t \neq 0$, $\tilde{r}_j(t)$ are uncorrelated, and they are added incoherently; and the sidelobes level is proportional to \sqrt{p} , then we can conclude that the signal/sidelobes is proportional to \sqrt{p} , that is to say, proportional to the square root of the total bandwidth of the transducer $ss_{TR} \propto \sqrt{\Delta\omega}$.

In Fig. 7(b), we measured experimentally the signal/sidelobes using different subbandwidths. Again, it is clear that the square root model is adequate. In order to have a very large bandwidth, we performed this experiment using wideband transducers of 3 MHz central frequency and 4.5 MHz bandwidth. Note that we cannot compare quantitatively both figures as these transducers are different from the ones used in Fig. 7(a). The signal/sidelobes for a time-reversal focusing has been shown to be proportional to:

$$ss_{TR} \propto \sqrt{\Delta\omega n}, \quad (6)$$

where $\Delta\omega$ is the bandwidth and n is the number of transducers.

Our goal is to estimate the signal/sidelobes for the PI technique ss_{PI} . The first harmonic generation results from a quadratic effect on the amplitude, this is clearly demonstrated in Fig. 7(c) in which the amplitude of the PI focusing grows following a quadratic behavior with respect to the amplitude of the classical time-reversal focusing. If the sidelobes follow the same quadratic behavior, we can conclude that $ss_{PI} = ss_{TR}^2$.

Thus, if we measure the signal/sidelobes in a decibel scale, the contrast obtained in a PI time-reversal process will be twice the one of the classical time-reversal experiment:

$$20 \log_{10} (cont_{PI}) = 2 \times 20 \log_{10} (cont_{TR}). \quad (7)$$

Fig. 7(d) shows the behavior of ss_{PI} versus ss_{TR} , both in a decibel scale. We clearly can see that ss_{PI} grows linearly in a decibel scale, but there is not exactly a factor of 2 as there is a difference of -12 dB between the estimates and the quadratic model. This difference is due to the errors introduced in the transmit mode by our electronics that are not accurate enough to send exactly the opposite pulse. Our electronics were not designed for PI, it has a nonlinear deviation in reception and it is not a high dynamical range.

III. IMAGE FORMATION USING THE CAVITY

In the previous sections, we presented in details the process of 3-D focusing in the transmit mode. In order to perform a pulse-echo imaging mode, a receiving mode also needs to be implemented. In most ultrasonic devices, the receiving transducers are the same as the transmit ones. However, in our case it is very difficult to use the same transducers in both transmit and receive modes. When the backscattered echoes reach the surface of the cavity, only a few percent of the pressure amplitude penetrates in the

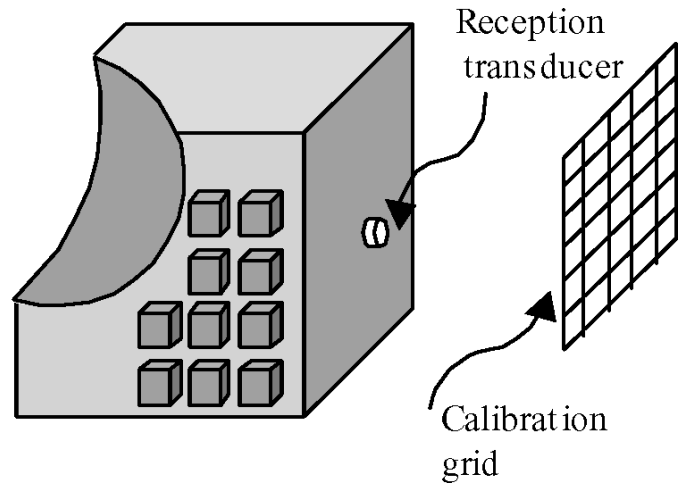


Fig. 8. Schema of the imaging method. One reception transducer is placed in the middle of the front face of the cavity. The calibration points are placed in a grid parallel to the front face.

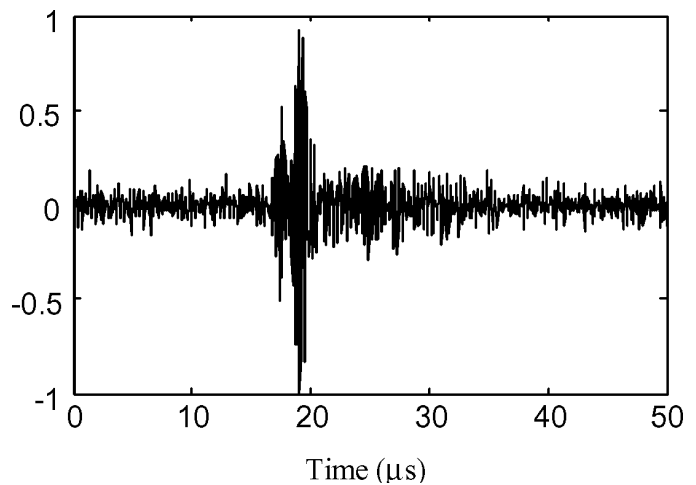


Fig. 9. Nonlinear pulse inversion echo of an object received by the front face receive transducer.

cavity because of the strong mechanical impedance mismatch between water and aluminum. As the reverberation time in the cavity is very long, these very weak backscattered echoes are mixed inside the cavity with the residual reverberation noise of the transmit sequence. Unfortunately, it is not possible to differentiate them from the latter. One might be tempted to decrease the impedance mismatch between the cavity and the imaged medium. However, such a choice would increase the leakage of waves out of the cavity during the transmit mode. Consequently, it would decrease the time-reversal focusing efficiency as the number of reverberations inside the cavity would be smaller.

Thus, the choice was done to use separate transmit and receive transducers. For the first step, a single receive transducer located in the center of the front face of the kaleidoscope (see Fig. 8) was chosen. The receive transducer is 0.5 mm in diameter to ensure a wide directivity pattern for detecting the backscattered echoes coming

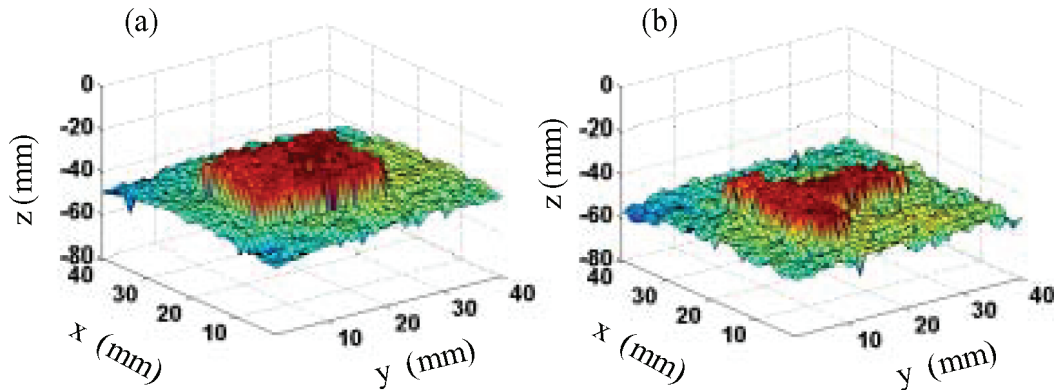


Fig. 10. Surface images of some objects obtained using a kaleidoscope made of only 31 emission transducers and a single reception transducer. (a) A rectangular object. (b) A T-shaped object.

from the largest volume of interest. The main advantages of this single receiver at the front face of the cavity is that it overcomes the limit of weak wave transmission at the solid-fluid interface. Backscattered echoes are recorded before entering the cavity. Moreover, the recorded signals are not disturbed by the disturbing noise of the initially transmitted echoes that reverberate during a long time in the cavity. And, the single receive element frequency is centered around the second harmonic component of the transmitted echoes in order to improve the separation between transmitted and backscattered echoes.

Thus, the final procedure in order to obtain an image consists in two steps:

- Calibration. The kaleidoscope is calibrated in water while learning the data set of transmit codes that allow us to focus pulses at any location in the 3-D volume of interest, as explained in Section II. Calibration experiments were carried out for 1600 focal points on a 40 by 40 grid, of a 40 by 40 mm plane placed at a 50 mm focal depth from the emitting surface (see Fig. 8). The 1600 codes were time reversed and stored using a 1-bit quantification.
- Imaging. The kaleidoscope then is placed in front of the object to image, and we measure the second harmonic component of the backscattered echoes using the single receive transducer. The test objects are tissue phantoms made of gelatin and containing randomly distributed scatterers (agar powder). An example of one backscattered echo is presented in Fig. 9. The noise induced by the sidelobes is of -25 dB, and we clearly can identify the echo of the object surface and some speckle noise coming from the phantom. An image of the object surface was made by measuring the different arrival times of the surface echoes (Fig. 10). These images are in good agreement with the real shape of the objects. The frame rate is limited by the spreading time in the cavity, using signals of $500 \mu\text{s}$ we need 0.8 seconds to make a 40 by 40 points image. The frame rate can be increased using only the first part of the signal, this generates a lower amplitude at the focus, but the 1-bit time reversal generates enough amplitude to make the image. The images of Fig. 10

are made using the first $200 \mu\text{s}$ of the emission signals, and we obtain three 3-D images/s. A second improvement can be implemented using a set of receptors and dynamical focusing, for example, it is possible to divide the image area in sectors and simultaneously send a focused pulse in a point of each sector by sending the sum of the signals to focus in each individual point.

The images obtained using this simple prototype made of only 31 emission transducers and 1 reception transducer are very encouraging as it can clearly detect a highly contrasted surface. However, the contrast is not yet high enough to image human organs. Using a single receiver means that there is no focus on receive, then it limits the resolution of the images. A kaleidoscope made of 64 emission transducers and 64 reception transducers is currently being designed and should lead to 3-D images of low contrasted objects using this new approach.

IV. CONCLUSIONS

In this article, we presented a new concept of a smart transducer able to generate 3-D ultrasonic images. Combined with the time-reversal process, this device exploits the multiple reverberations in a chaotic and leaky cavity to focus a pulse in the medium of interest.

Taking advantage of the nonlinear propagation, the PI technique permits a high quality focusing as it eliminates the undesired low level temporal and spatial sidelobes. Using a pioneer prototype made of only 31 emission transducers and a single reception transducer, we were able to image the 3-D surface of some objects. It is important to note that such chaotic cavities are very easy to build; we do not need to use small transducers or specific shapes, we can glue transducers everywhere on the external surface of the cavity. A mechanical layer matching is not needed. On the contrary, the mechanical impedance mismatch between the cavity and the imaged medium is responsible for the ability of time-reversal processing to focus waves in a 3-D volume with a very small number of transducers. Compared to the technological difficulties of a 2-D

array of transducers, these simplifications make the construction of the cavities very easy. The complexity of 2-D arrays design is now transferred into the spatiotemporal coding techniques adapted to the cavity shape and stored into memories.

REFERENCES

- [1] T. R. Nelson and D. H. Pretorius, "Three-dimensional ultrasound imaging," *Ultrasound Med. Biol.*, vol. 24, no. 9, pp. 1243–1270, 1998.
- [2] A. Fenster and D. B. Downey, "3-D Ultrasound imaging: A review," *IEEE Eng. Med. Biol.*, vol. 15, pp. 41–51, 1996.
- [3] K. Baba, K. Satoh, S. Sakamoto, O. Takashi, and S. Ishii, "Development of an ultrasonic system for three-dimensional reconstruction of the fetus," *J. Perinat. Med.*, vol. 17, pp. 19–24, 1989.
- [4] T. R. Nelson and D. H. Pretorius, "Interactive acquisition, analysis, and visualization of sonographic volume data," *Int. J. Imaging Syst. Technol.*, vol. 8, pp. 26–37, 1997.
- [5] E. D. Light, R. E. Davidsen, J. O. Fiering, T. A. Hruschka, and S. W. Smith, "Progress in two dimensional arrays for real time volumetric imaging," *Ultrason. Imag.*, vol. 20, pp. 235–250, 1998.
- [6] J.-Y. Lu and J. F. Greenleaf, "A study of two-dimensional array transducers for limited diffraction beams," *IEEE Trans. Ultrason., Ferroelect., Freq. Contr.*, vol. 41, pp. 724–739, 1994.
- [7] R. E. Davidsen, J. A. Jensen, and S. W. Smith, "Two-dimensional random arrays for real time volumetric imaging," *Ultrason. Imag.*, vol. 16, pp. 143–163, 1994.
- [8] S. W. Smith, G. E. Trahey, and O. T. von Ramm, "Two-dimensional arrays for medical ultrasound," *Ultrason. Imag.*, vol. 14, pp. 213–233, 1992.
- [9] M. Fink, "Time reversed acoustics," *Phys. Today*, vol. 50, pp. 34–40, 1997.
- [10] M. Fink, G. Montaldo, and M. Tanter, "Time reversal acoustics in biomedical engineering," *Annu. Rev. Biomed. Eng.*, vol. 5, pp. 465–497, 2003.
- [11] H. C. Song, W. A. Kupperman, W. S. Hoogkiss, T. Akal, and C. Ferla, "Iterative time reversal in the ocean," *J. Acoust. Soc. Amer.*, vol. 105, pp. 3176–3184, 1999.
- [12] G. Montaldo, P. Roux, A. Derode, C. Negreira, and M. Fink, "Ultrasonic shock wave generator using 1-bit time-reversal in a dispersive medium: Application to lithotripsy," *Appl. Phys. Lett.*, vol. 80, no. 5, pp. 897–899, 2002.
- [13] C. Draeger and M. Fink, "One channel time-reversal of elastic waves in a chaotic 2-D-silicon cavity," *Phys. Rev. Lett.*, vol. 79, no. 3, pp. 407–410, 1997.
- [14] C. Draeger, J.-C. Aime, and M. Fink, "One-channel time-reversal in chaotic cavities: Experimental results," *J. Acoust. Soc. Amer.*, vol. 105, no. 2, pp. 618–625, 1999.
- [15] A. Derode, A. Tourin, and M. Fink, "Ultrasonic pulse compression with one-bit time reversal through multiple scattering," *J. Appl. Phys.*, vol. 85, no. 9, pp. 6343–6352, 1999.
- [16] T. Christopher, "Experimental investigation of finite amplitude distortion based, second harmonic pulse echo ultrasonic imaging," *IEEE Trans. Ultrason., Ferroelect., Freq. Contr.*, vol. 45, no. 1, pp. 158–162, 1998.
- [17] B. Ward, A. C. Baker, and V. F. Humphrey, "Nonlinear propagation applied to the improvement of resolution in diagnostic medical ultrasound," *J. Acoust. Soc. Amer.*, vol. 101, no. 1, pp. 143–154, 1997.
- [18] M. A. Averkiou and M. F. Hamilton, "Measurements of harmonic generation in a focused finite-amplitude sound beam," *J. Acoust. Soc. Amer.*, vol. 98, pp. 3439–3442, 1995.
- [19] P. N. Burns, "Harmonic imaging with ultrasound contrast agents," *Clin. Radiol.*, vol. 51, no. 1, pp. 50–55, 1996.
- [20] P. H. Chang, K. K. Shung, S. Wu, and H. B. Levene, "Second harmonic imaging and harmonic Doppler measurements with Alunex," *IEEE Trans. Ultrason., Ferroelect., Freq. Contr.*, vol. 42, no. 6, pp. 1020–1027, 1995.
- [21] A. Derode, A. Tourin, J. de Rosny, M. Tanter, S. Yon, and M. Fink, "Taking advantage of multiple scattering to communicate

with time reversal antennas," *Phys. Rev. Lett.*, vol. 90, no. 1, pp. 014301-1–014301-4, 2003.



Gabriel Montaldo was born 1972 in Montevideo, Uruguay. He received the Ph.D. degree in physics from the Universidad de la Republica, Uruguay, in 2001. Since 2002 he has worked in the Laboratory Ondes et Acoustique at the Ecole Supérieure de Physique et de Chimie Industrielles de la Ville de Paris (ESPCI).

His principal research includes applications of the time-reversal process to adaptive focusing in heterogeneous media, the generation of shocks waves, and telecommunications.



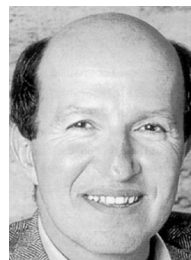
Delphine Palacio was born in June 1976 in Créteil, France. In 2002 she was successful on a competitive exam to be a physics teacher. In 2001 she was student at the Ecole Normale de Cachan (ENS Cachan) and she received the engineer degree from the Ecole Supérieure de Physique et de Chimie Industrielles de la Ville de Paris (ESPCI) with a specialization in physics. In 2000, she received her master's degree at the Laboratoire Ondes et Acoustique in Paris. She is now achieving her Ph.D. degree at the Laboratoire Ondes et Acoustique,

working on 3-D echographic imaging using chaotic cavities.



Mickael Tanter was born in December 1970 in Paimpol, France. He received the engineer degree in Electronics of SUPELEC in 1994. In 1999, he received the Ph.D. degree in physics (Acoustics) from the University of Paris VII for his work on the application of time reversal to ultrasonic brain hyperthermia. He is now a researcher in the National French Center of Science (C.N.R.S.) and in 2000 joined the laboratory Ondes et Acoustique at the Ecole Supérieure de Physique et de Chimie Industrielle de la ville de Paris (ESPCI). His current

research interests include wave focusing techniques in heterogeneous media, medical ultrasonic imaging, ultrasonic brain imaging, shear wave propagation in soft tissues for cancer detection, ultrasonic therapy, nonlinear acoustics, active noise control.



Mathias Fink received the diplome de Doctorat de 3^{ème} cycle in solid state physics in 1970 and the Doctorat ès-Sciences degree in acoustics in 1978 from Paris University, France.

From 1981 to 1984, he was a professor of acoustics at Strasbourg University, Srasbourg, France. Since 1984, he has been a professor of physics at Paris University, Denis Diderot, France. In 1990 he founded the Laboratoire Ondes et Acoustique at the Ecole Supérieure de Physique et de Chimie Industrielles de la

Ville de Paris (ESPCI). In 1994, he was elected a member of the Institut Universitaire de France.

His current research interest include medical ultrasonic imaging, ultrasonic therapy, nondestructive testing, underwater acoustics, active control of sound and vibration, analogies between optics and acoustics, wave coherence in multiple scattering media, and time reversal in physics. He has developed different techniques in speckle reduction, wave focusing in inhomogeneous media, and in ultrasonic laser generation. He holds 20 patents, and he has published more than 220 articles. In 2003, he was elected a member of the French Academy of Science.